

2020-02-17

Multiscale Simulations of New Coronavirus

1

2

3 **A Multiscale and Comparative Model for Receptor Binding of 2019**

4 **Novel Coronavirus and the Implication of its Life Cycle in Host Cells**

5

6 Zhaoqian Su¹ and Yinghao Wu^{1,*}

7 ¹Department of Systems and Computational Biology, Albert Einstein College of

8 Medicine, 1300 Morris Park Avenue, Bronx, NY, 10461

9

10

11

12

13

14

15 *Corresponding authors:

16 Yinghao Wu

17 Phone: (718) 678-1232, Fax: (718) 678-1018, E-mail: yinghao.wu@einstein.yu.edu

2020-02-17

Multiscale Simulations of New Coronavirus

1 **ABSTRACT**

2 The respiratory syndrome caused by a new type of coronavirus has been emerging from
3 China and caused more than 1000 death globally since December 2019. This new virus,
4 called 2019 novel coronavirus (2019-nCoV) uses the same receptor called Angiotensin-
5 converting enzyme 2 (ACE2) to attack humans as the coronavirus that caused the severe
6 acute respiratory syndrome (SARS) seventeen years ago. Both viruses recognize ACE2
7 through the spike proteins (S-protein) on their surfaces. It was found that the S-protein
8 from the SARS coronavirus (SARS-CoV) bind stronger to ACE2 than 2019-nCoV.
9 However, function of a bio-system is often under kinetic, rather than thermodynamic,
10 control. To address this issue, we constructed a structural model for complex formed
11 between ACE2 and the S-protein from 2019-nCoV, so that the rate of their association
12 can be estimated and compared with the binding of S-protein from SARS-CoV by a
13 multiscale simulation method. Our simulation results suggest that the association of new
14 virus to the receptor is slower than SARS, which is consistent with the experimental data
15 obtained very recently. We further integrated this difference of association rate between
16 virus and receptor into a mathematical model which describes the life cycle of virus in
17 host cells and its interplay with the innate immune system. Interestingly, we found that
18 the slower association between virus and receptor can result in longer incubation period,
19 while still maintaining a relatively higher level of viral concentration in human body. Our
20 computational study therefore provides, from the molecular level, one possible
21 explanation that the new disease by far spread much faster than SARS.

22

23

24

25

26

27

2020-02-17

Multiscale Simulations of New Coronavirus

1 **Introduction**

2 The coronavirus disease 2019 (COVID-19) has emerged at the end of year 2019
3 from Wuhan, a city in China, as a new infectious disease [1, 2]. It has been found that the
4 disease is caused by a new member of coronavirus family, 2019-nCoV [3, 4]. Like others
5 in the same virus family, such as the coronavirus causing SARS [5, 6], 2019-nCoV is a
6 single and positive-stranded RNA virus enveloped by lipid bilayer. The virus can capture
7 and enter host cells in human through targeting specific receptors on their surface. Upon
8 entry, the viral genome is released through membrane fusion. The released RNA genome
9 of the virus is then replicated and translated into various types of viral proteins. The
10 replicated RNA genome and synthesized viral proteins are finally assembled together into
11 new viruses, before they escape and attack other cells [7, 8]. As a result, the infections of
12 2019-nCoV normally come with the similar symptoms as SARS, including fever,
13 respiratory difficulty and pneumonia [9, 10]. Different from SARS, however, the new
14 COVID-19 seems to have longer incubation period and thus is more contagious [11]. The
15 disease has caused more than 70,000 confirmed cases with at least 1000 death globally,
16 according to the data from the World Health Organization (WHO) on February 16th 2020.
17 Therefore, the development of vaccine or therapeutic treatment for this ongoing public
18 health crisis is highly demanding [12, 13].

19 Almost all the coronaviruses recognize their host cells through spike (S) proteins
20 [14, 15]. S-protein is a glycoprotein expressed on the surface of viral envelop as homo-
21 trimers [16]. Each S-protein further consists of two subunits. The S1 subunit includes a
22 region called receptor-binding domain (RBD) which is used to target receptors in host
23 cells, while the S2 subunit regulates the membrane fusion between virus and host cells
24 [17]. These roles of S protein suggest that it could be a key target for vaccine and
25 therapeutics developed to neutralize virus infection by blocking their invasion [18].
26 Moreover, it has been confirmed in a recent report that the new virus 2019-nCoV uses the
27 same cell entry receptor ACE2 as SARS coronavirus [19]. The atomic structures of
28 complex between human ACE2 and the RBD regions from S-protein of SARS-CoV have
29 been obtained by x-ray crystallography [17]. It was also shown that the sequence of S-
30 protein from SARS-CoV shares more than 70% identity with the S-protein from 2019-

2020-02-17

Multiscale Simulations of New Coronavirus

1 nCoV [6]. Therefore, it is reasonable to hypothesize that the new coronavirus uses the
2 similar binding interface with ACE2 as SARS to enter host cells of human. The obvious
3 follow-up questions are: whether the 30% variations in sequences between S-protein of
4 2019-nCoV and SARS can cause any difference in their binding to ACE2? Moreover,
5 does this difference lead into any functional impacts on the life cycles of these viruses in
6 host cells?

7 Comparing with the time-consuming and labor-expensive experimental studies,
8 computational modeling serves as an ideal alternative approach to carry out fast tests on
9 biological systems under the conditions that are currently inaccessible in the laboratory
10 [20-26]. Therefore, here we developed a multiscale computational strategy to compare
11 the process of recognition between the SARS-CoV and host cells with the interactions
12 between the new coronavirus and host cells. A mesoscale model is used to simulate the
13 process in which the coronaviruses are captured by ACE2 receptors on cell surface. We
14 further constructed a structural model for complex formed between ACE2 and RBD of
15 2019-nCoV S-protein, so that the rate of their association can be estimated by a coarse-
16 grained Monte-Carlo simulation and further compared with the binding of S-protein from
17 SARS-CoV. Our simulation indicates that association of the new virus to the receptor is
18 slower than SARS, which is consistent with the experimental data obtained very recently.
19 We integrated this difference of association rate between virus and receptor into a simple
20 mathematical model which describes the life cycle of virus in host cells and its interplay
21 with the innate immune system. Interestingly, we found that the slower association
22 between virus and receptor can result in longer incubation period, while still maintaining
23 a relatively higher level of viral concentration in human body. Our computational study
24 therefore explains, from the molecular level, why the new COVID-19 disease is by far
25 more contagious than SARS. In summary, this multiscale model serves as a useful
26 addition to current understanding for the spread of coronaviruses and related infectious
27 agents.

28 **Results and Discussions**

29 A rigid-body (RB) based model is first constructed to simulate the kinetic process
30 about how viruses are captured by the cell surface receptors on plasma membrane. In

2020-02-17

Multiscale Simulations of New Coronavirus

1 brief, within a three-dimensional simulation box, the plasma membrane is represented by
2 a flat surface below the extracellular region. The area of the square is $1 \mu\text{m}^2$, while the
3 height of the simulation box is 500 nm. A number of ACE2 receptors (200) are initially
4 placed on the membrane surface (pink in **Figure 1a**). They are represented by rigid
5 bodies of cylinders and their binding sites are located on top of the cylinders (red dots in
6 **Figure 1a**). The height of each cylinder is 10nm and its radius is 5nm. On the other hand,
7 space above the plasma membrane represents the extracellular region. A number of
8 coronaviruses are located in this area (golden in **Figure 1a**). Each virus is simplified as a
9 spherical rigid body with a given radius (40nm). Trimeric S-proteins are uniformly
10 distributed on the spherical surface of each virus (green dots in **Figure 1a**). Each S-
11 protein can interact with an ACE2 receptor on plasma membrane. After any S-protein on
12 one virus forms an encounter complex with a receptor, we assume that the host cell is
13 captured by the virus. The dissociation between the virus and the receptor is not
14 considered in the system, because we also assume that, after the association between S-
15 protein and ACE2, the virus can enter the cell through membrane fusion. Following the
16 initial random configuration, the diffusion of receptors and viruses, as well as their
17 association, were simulated by a diffusion-reaction algorithm until the system reached
18 equilibrium. The detail process of the simulation is specified in the **Methods**.

19 Before the rigid-body simulation, in order to provide a more realistic estimation
20 on the binding between ACE2 and different coronaviruses, we specifically compared the
21 S-protein from 2019-nCoV with the S-protein from SARS. We applied our previously
22 developed residue-based kinetic Monte-Carlo (KMC) method to simulate the associate
23 processes of these two systems. In detail, the atomic coordinates of the complex between
24 human ACE2 and the RBD domain from the S-protein of SARS are taken from the PDB
25 id 2AJF [17]. In parallel, the structural model of the complex between human ACE2 and
26 the RBD domain from the S-protein of 2019-nCoV was computationally constructed,
27 following the procedure described in the **Methods**. The structural comparison of these
28 two protein complexes is shown in **Figure 1b**. For both systems, 500 trajectories based
29 on their complex structures were generated by the KMC simulation which algorithm is
30 specified in the **Methods**. In the initial conformation of each trajectory, S-protein and
31 receptor were separated and placed with a random position relative to each other in which

2020-02-17

Multiscale Simulations of New Coronavirus

1 the distance between their binding interfaces is fallen within a given cutoff value d_c of 20
2 Å. At the end of each trajectory, receptor and viral protein either form an encounter
3 complex through their binding interface observed in the complex structure, or diffuse
4 away from each other. Based on the simulation results collected from all the 500
5 trajectories, we counted how many times an encounter complex can be formed by the end
6 of the simulation time, which gives the probability of association. As a result, the
7 comparison of calculated probabilities of association for both systems is plotted in **Figure**
8 **2a**.

9 The figure shows that probability of association between ACE2 and the S-protein
10 from 2019-nCoV is remarkably lower than the probability of association between ACE2
11 and the S-protein from SARS. Specifically, among the 500 simulation trajectories of
12 SARS system, we found that 8 of them successfully formed encounter complexes, while
13 among the 500 simulation trajectories of 2019-nCoV system, only 2 of them successfully
14 formed encounter complexes. This result suggests that the association of the S-protein
15 from SARS to the receptor is about four times faster than the association of the S-protein
16 from 2019-nCoV. The different of association rate from our simulation, interestingly, is
17 confirmed by the experimental data that was measured very recently by Dr. McLellan's
18 lab [27]. Using surface plasma resonance (SPR), they showed that the association rate k_a
19 of binding between 2019-nCoV RBD domain and ACE2 equals $1.36 \times 10^5 \text{M}^{-1} \text{s}^{-1}$, while the
20 rate between SARS RBD domain and ACE2 equals $3.62 \times 10^5 \text{M}^{-1} \text{s}^{-1}$. Therefore, the
21 experimental evidence indicated that the association of the S-protein from SARS to the
22 receptor is about three times faster than the association of the S-protein from 2019-nCoV,
23 which is quantitatively consistent with our simulation results.

24 We then fed the information derived from the structure-based simulations into the
25 rigid-body model. Two specific simulation systems were compared. A relatively fast rate
26 of association between receptors and S-proteins on viral surfaces was adopted in the first
27 system to represent the binding process of SARS, while a relatively slow rate of
28 association between receptors and S-proteins on viral surfaces was adopted in the second
29 system to represent the binding process of 2019-nCoV. All the other parameters such as
30 diffusion constants and concentrations in both systems remain the same. As a result, the

2020-02-17

Multiscale Simulations of New Coronavirus

1 total numbers of viruses that were captured by host cells are plotted in **Figure 2b** as a
2 function of simulation time. Without surprise, the figure shows that although almost all
3 viruses were attached to the cell surfaces by the end of both simulations, the kinetic
4 process in the SARS system is much faster than the 2019-nCoV system, which is resulted
5 from the difference in the association rate between receptors and their corresponding S-
6 proteins. This leads into the fact that during the early stage of simulations, more SARS
7 viruses attach to host cells than 2019-nCoV. For instance, when the simulations in both
8 systems reached the first 10^5 nanoseconds, there have already been more than 40 SARS
9 viruses attached to the cell surfaces. In contrast, there were less than 20 viruses attached
10 to the cell surfaces within the same amount of time in the 2019-nCoV system.
11 Considering that the function of a bio-system is often under kinetic, rather than
12 thermodynamic, control [28, 29], we suggest that this time-dependent behavior is
13 biologically more relevant. In reality, not all the viruses have the opportunity to find their
14 target receptors on host cells. Many of them will be recognized and removed by our
15 innate immune system. Therefore, the capability of how fast a specific type of
16 coronavirus can target its receptors is especially critical to the process of its invasion, as
17 well as the follow-up stages in its life cycle.

18 In order to further explore the impacts of our rigid-body simulation results on the
19 rest process of virus infection after they invade into host cells, we proposed a
20 mathematical model to delineate a simplified version of viral life cycle including its
21 replication and packaging in host cells, the inflammatory signaling pathways due to the
22 detection of foreign pathogens, and the follow-up inflammatory responses which lead to
23 the apoptosis of infected cells and the removal of viruses by the recruitment of immune
24 cells. The model can be summarized by the diagram shown in **Figure 3**. Specifically,
25 coronavirus [V] can turn healthy cells [H] into infected cell [In] by binding to the
26 receptors ACE2 on their surfaces. The RNA genome [m] is then released from bound
27 virus [Vb], and then translated into different viral proteins. These proteins and replicated
28 RNA are further packaged together as [P] in cytoplasm and finally escape from infected
29 cells. On the other side, in order to avoid viral spread, our innate immune system triggers
30 inflammatory signaling pathways in the infected cells [30]. For instance, the viral RNAs
31 can be detected by RIG-I-like receptors (RLRs) [31]. The RNA binding of RLRs

2020-02-17

Multiscale Simulations of New Coronavirus

1 receptors initiates the signaling cascade by interacting with the mitochondrial antiviral-
2 signaling (MAVS) protein [32]. The aggregation of MAVS on the surface of
3 mitochondria will trigger the NF- κ B signaling pathway that turns on gene expression of
4 specific cytokines [S] to stimulate the inflammatory responses [33, 34]. The inflammation
5 of host organism leads to the apoptosis of infected cells and the removal of virus by
6 recruited immune cells such as microphages. In summary, the change of concentration for
7 each variable in above system can be described by following set of ordinary differential
8 equations (ODE).

9
$$\frac{d[H]}{dt} = r_H - \frac{k_b [H][V]}{S_V + [V]} \quad (1)$$

10
$$\frac{d[Vb]}{dt} = \frac{k_b [H][V]}{S_H + [H]} - k_r [Vb] \quad (2)$$

11
$$\frac{d[m]}{dt} = k_r [Vb] - k_p [m] \quad (3)$$

12
$$\frac{d[P]}{dt} = k_p [m] - k_a [P] \quad (4)$$

13
$$\frac{d[S]}{dt} = \frac{s_s [m]}{[m] + K_m} - d_s [S] \quad (5)$$

14
$$\frac{d[In]}{dt} = \frac{k_b [H][V]}{S_V + [V]} - \frac{d_I [In][S]}{[In] + K_I} \quad (6)$$

15
$$\frac{d[V]}{dt} = k_a [P] - \frac{k_b [H][V]}{S_H + [H]} - \frac{d_v [V][S]}{K_V + [V]} \quad (7)$$

16 Equation (1) describes the change of the healthy cells as a function of time in the
17 system. The parameters r_H , k_b , and S_V in the equation represent cell generating rate, the
18 rate and saturation coefficient of virus binding, respectively. Equations (2) to (4) indicate
19 the entry, replication and packaging of virus in host cells, in which the parameters k_r , k_p ,
20 and k_a represent rates of viral protein translation, assembly and releasing. Equation (5)

2020-02-17

Multiscale Simulations of New Coronavirus

1 describes the stimulation of inflammatory signaling by viral RNA. The parameters s_S , K_m ,
2 and d_S in the equation represent the maximal activation rate, the saturation coefficient and
3 the rate of degradation of inflammatory signals. Equation (6) gives how infected cells
4 change in the system, while the parameters in the equation d_I , and K_I indicate the rate and
5 saturation coefficient of cell apoptosis that is stimulated by inflammatory signals. Finally,
6 equation (7) suggests that the variation of total virus in the system depends on the release
7 of newly packaged virus from infected cells, the binding of free virus to the healthy cells,
8 and the immune response triggered by inflammatory signals. The parameters d_V and K_V in
9 the equation give the maximal rate and saturation coefficient immune cells used to kill
10 virus. Altogether, we solved above ODEs numerically by a stochastic simulation
11 algorithm. The brief introduction of the simulation algorithm will be specified in the
12 **Methods**.

13 Given predefined weights for all the simulation parameters and the initial values
14 for each element, the dynamics of the system is evolved as a function of time. The
15 simulation results of the mathematical model are summarized in **Figure 4**. As shown by
16 the red curve in **Figure 4a**, the change of free virus in the system can be divided into
17 three stages. It first decreases from its initial value. After reaching the minimal level, the
18 number of virus then bounces back in the second phase until it drops again and finally
19 vanishes at the end of the third phase. Relative to the free virus, the number of virus
20 captured by host cells equals 0 at the beginning of the simulation. It increases in the first
21 stage and diminishes in the second, as shown by the blue curve in the figure. In the third
22 phase, very few viruses bound to host cells are detected in the system. Corresponding to
23 the change of virus, the number of healthy cells is plotted as the black curve. The curve
24 shows that the level of healthy cells reduces from the beginning and rises only after all
25 free viruses are removed from the systems. Based on these kinetic profiles, the dynamics
26 of the system can thus be interpreted as follows. In the first stage of simulation, free
27 viruses invade into the healthy cells by binding to the receptors on their surface. We
28 suggest that this stage corresponds to the incubation period. In the second stage, new
29 viruses are assembled in and released from the infected cells. At the same moment, the
30 viral genomes left in the infected cells stimulate the immune response. As a result, the
31 total amount of virus is gradually lowered in the third phase, indicating that these viruses

2020-02-17

Multiscale Simulations of New Coronavirus

1 are cleared up by the innate immune system. After the removal of all viruses, the healthy
2 cells in the system grow again, representing the recovery of the patient.

3 We further incorporated the results derived from the rigid-body simulations into
4 the mathematical model to compare the viral life cycle in SARS and COVID-19. The
5 rigid-body simulation suggests that SARS-CoV binds to receptor ACE2 faster than 19-
6 nCoV, given the same amount of time. Therefore, we applied the mathematical model to
7 two comparative systems. A relatively fast viral binding rate k_b was adopted in the first
8 system to represent the binding process of SARS, while a relatively slow rate was
9 adopted in the second to represent the binding process of 2019-nCoV. All the other
10 parameters such as diffusion constants and concentrations in both systems remain the
11 same. As a result, the kinetic profiles indicating the changes of free virus level along with
12 the simulation time in these two systems are shown in **Figure 4b**. The figure suggests
13 that the first stage in the simulation of 2019-nCoV (red curve) is longer than the
14 simulation of SARS (black curve). This is consistent with the clinical observation that the
15 incubation period of COVID-19 could be as long as 14 days, while the incubation period
16 is normally from 2 to 7 days. More interestingly, we found that the level of free virus at
17 the end of the first period in the simulation of 2019-nCoV is relatively higher than the
18 corresponding level of free virus in the simulation of SARS. Considering that a patient
19 can contain a higher level of new coronavirus during his or her incubation period which
20 is also longer than SARS, our simulation gives the insights about why COVID-19 is more
21 contagious and spread faster than SARS [11]. Finally, when both simulations came to
22 their third phases, we found that the total amount of virus of SARS is higher than 2019-
23 nCoV. This gives possible explanation about why the symptoms in most COVID-19
24 patients are relatively mild and not as severe as the symptoms in SARS patients [35].

25 In summary, it is important to point out that the life cycles of different
26 coronaviruses can also be caused by many other factors such as the difference in the
27 assembling pathways of these viruses. Additionally, the infectious response of each
28 individual is also a case-dependent issue, relying on the expression levels of ACE2
29 receptors and the heterogeneity of immune response in different patients. Nevertheless,
30 our multiscale computational model highlights the potential role of binding kinetics

2020-02-17

Multiscale Simulations of New Coronavirus

1 between human receptor and S-proteins from different coronavirus in, and provided the
2 possible mechanism from the molecular level to their impacts on, regulating the
3 dynamics of the entire viral life cycle.

4 **Conclusions**

5 The recent outbreak of COVID-19 has drawn substantial attention especially after
6 it spread to more than thirty countries and became a Public Health Emergency of
7 International Concern (PHEIC) [2, 36, 37]. The disease is caused by a new type of
8 positive-stranded RNA virus, known as 2019-nCoV. Similar as the coronavirus that leads
9 to SARS, it has been confirmed that the S-protein in 2019-nCoV also mediates its
10 recognition with the human receptor ACE2. However, the differences of receptor binding
11 in these two virus systems and their underlying implications are not well understood. It
12 has been found that the kinetic aspect of binding between biomolecules in many
13 biological systems is usually more important to their functions. Here, using
14 computational structural prediction and coarse-grained simulations, we first have
15 compared the association rate of binding between ACE2 and the S-protein from SARS-
16 CoV with binding between ACE2 and the S-protein from 2019-nCoV. Consistent with
17 the experimental data obtained very recently, we found association of the new virus to the
18 receptor is slower than SARS. We further interrogate the impact of this result on the
19 difference in viral life cycle between SARS and COVID-19. By incorporating the
20 information derived from coarse-grained simulations into a mathematical model, we
21 found that the slower association between 2019-nCoV and ACE2 can result in longer
22 incubation period, while still maintaining a relatively higher level of viral concentration
23 in human body. This multiscale modeling framework, therefore, can offer one possible
24 molecular mechanism to explain why this new infectious disease spreads much faster
25 than SARS.

26 **Methods**

27 *Construct the structural models for the complexes between receptors and viral S-proteins*

28 The atomic structures of complex between ACE receptor and different viral S-
29 proteins are needed for the simulations of their association. The structural models of these

2020-02-17

Multiscale Simulations of New Coronavirus

1 protein complexes were prepared as follows. The complex structure between human
2 ACE2 and the RBD domain from the S-protein of SARS was determined by the x-ray
3 crystallography experiment (PDB id 2AJF) [17]. On the other hand, the structural model
4 of the complex between human ACE2 and the RBD domain from the S-protein of 2019-
5 nCoV was constructed by computational modeling. In detail, the atomic structure of
6 2019-nCoV S-protein RBD domain was first predicted by I-TASSER [38] based on the
7 newly released sequence of 2019-nCoV [39]. In parallel, the backbone model of the
8 complex between human ACE2 and the RBD domain from 2019-nCoV S-protein was
9 generated using the template-based structure prediction tool COTH [40, 41]. We then
10 superimposed the predicted atomic coordinates of 2019-nCoV S-protein RBD domain
11 onto its relative backbone position in the complex model, and also aligned the atomic
12 coordinates of human ACE2 from the crystal structure onto the relative backbone
13 position in the complex model. As a result, the structural comparison of these two protein
14 complexes is plotted in **Figure 1b**.

15 *Estimate the association between ACE2 and S-protein by kinetic Monte-Carlo simulation*

16 A previously developed kinetic Monte-Carlo algorithm [42] was used to simulate
17 the association between S-protein and ACE2. A coarse-grained model of protein
18 structures is used. Each residue in a protein is represented by its $C\alpha$ atom and the
19 representative center of its side-chain. The simulation starts from an initial conformation,
20 in which two proteins in the complex are separated and placed randomly. Following the
21 initial conformation, each protein diffuses randomly within one simulation step. A
22 physics-based scoring function containing electrostatic interaction and hydrophobic effect
23 is used to guide the diffusions of proteins during simulations. Based on the calculated
24 energy, Metropolis criterion is applied to determine if the corresponding diffusional
25 movements can be accepted or not. The simulation trajectory will be terminated if an
26 encounter complex is successfully formed through the corresponding interface observed
27 in the constructed model of native protein complexes. Otherwise, above simulation
28 procedure will be repeated until it reached the maximal time duration. This method was
29 applied to study the association between ACE2 and both S-proteins from the two virus
30 systems. For each system, 500 trajectories are carried out. Each trajectory starts from a

2020-02-17

Multiscale Simulations of New Coronavirus

1 relatively different initial conformation, but the initial distances between the binding
2 interfaces of S-proteins and receptors in all trajectories are below 20Å. The probabilities
3 of association were then derived and compared based on counting how many encounter
4 complexes formed among these trajectories in the two systems.

5 *Model the cellular attachment of coronavirus by rigid-body diffusion-reaction algorithm*

6 As described in the **Results**, a rigid-body (RB) based model is constructed to
7 simulate the binding between coronaviruses and cell surface receptors ACE2 on plasma
8 membrane. Given the model representation and a randomly-generated initial
9 configuration (**Figure 2a**), the dynamics of the system is evolved by following a
10 diffusion-reaction algorithm [43-45]. Viruses or receptors are selected by random order
11 for stochastic diffusion within each simulation time step. A virus is free to diffusion
12 throughout the simulation box, while diffusions of membrane-bound receptors are
13 confined to the plasma membrane. Periodic boundary conditions along both x and y
14 directions are applied. Moreover, viruses are not allowed to move below the plasma
15 membrane. If any virus moves beyond the top of the simulation box, it will be bounced
16 back. The amplitude and probability of translational and rotational movements for viruses
17 and receptors are determined by its corresponding diffusion constant. Association
18 between viruses and receptors are followed after diffusions. Association is triggered if the
19 distance between any S-protein in a virus and the binding site of a receptor is below a
20 predetermined cutoff value. The probability to trigger the association is determined by
21 the association rate, which was estimated by the kinetic Monte-Carlo method described in
22 the previous section. Assuming that viruses can enter the cell through membrane fusion
23 after they associate with ACE2, the dissociation between the virus and the receptor is not
24 considered in the system. Finally, as above diffusion-reaction process iterates in both
25 Cartesian and compositional spaces, the system will finally reach equilibrium.

26 *Solve the ordinary differential equations of viral life cycle by stochastic simulations*

27 We use the stochastic simulation algorithm (SSA) developed by Gillespie to
28 model the processes of biochemical reactions from equation (1) to equation (7) [46]. The
29 algorithm starts from the initiation of time and populations of each species in the

2020-02-17

Multiscale Simulations of New Coronavirus

1 simulation system. Within each simulation step, the rates for all reactions are re-estimated
2 by the given parameters and updated population of corresponding species. One of these
3 reactions is then randomly selected based on the calculation of their relative weights.
4 Finally, populations for the corresponding species are updated. The simulation moves
5 forward to the next step by adding the system time with τ , in which τ is an exponential
6 random variable with the average value equals the reciprocal of the summation for all the
7 reactions. Above process is iterated so that the populations of each species in the system
8 evolve along the simulation time. The values of all parameters in the simulation were
9 chosen to be within the biologically meaningful range. The choice of these parameters
10 does not qualitatively affect the general dynamic patterns of the system.

11

12

13

14

15

16

17

18

19

20

21

22

23

24

25

26

27

28

29

30

31

2020-02-17

Multiscale Simulations of New Coronavirus

1 **Acknowledgement**

2 This work was supported by the National Institutes of Health under Grant Numbers
3 R01GM120238 and R01GM122804. The work is also partially supported by a start-up
4 grant from Albert Einstein College of Medicine. Computational support was provided by
5 Albert Einstein College of Medicine High Performance Computing Center.

6

7 **Author Contributions**

8 Y.W. designed research; Z.S. and Y.W. performed research; Z.S. and Y.W. analyzed data;
9 Y.W. wrote the paper.

10

11 **Declaration of Interests**

12 **Competing financial interests:** The authors declare no competing financial interests.

13

14

15

16

17

18

19

20

21

22

23

24

25

26

27

28

29

1 References

- 2 1. Huang, C., et al., *Clinical features of patients infected with 2019 novel coronavirus in*
3 *Wuhan, China*. Lancet (London, England), 2020. **395**(10223): p. 497-506.
- 4 2. Chan, J.F.-W., et al., *A familial cluster of pneumonia associated with the 2019 novel*
5 *coronavirus indicating person-to-person transmission: a study of a family cluster*. Lancet
6 (London, England), 2020. **395**(10223): p. 514-523.
- 7 3. Carlos, W.G., et al., *Novel Wuhan (2019-nCoV) Coronavirus*. American journal of
8 respiratory and critical care medicine, 2020. **201**(4): p. P7-P8.
- 9 4. The, L., *Emerging understandings of 2019-nCoV*. Lancet (London, England), 2020.
10 **395**(10221): p. 311-311.
- 11 5. Wu, F., et al., *A new coronavirus associated with human respiratory disease in China*.
12 Nature, 2020: p. 10.1038/s41586-020-2008-3.
- 13 6. Lu, R., et al., *Genomic characterisation and epidemiology of 2019 novel coronavirus:*
14 *implications for virus origins and receptor binding*. Lancet (London, England), 2020: p.
15 S0140-6736(20)30251-8.
- 16 7. Qin, P., et al., *Characteristics of the Life Cycle of Porcine Deltacoronavirus (PDCoV) In*
17 *Vitro: Replication Kinetics, Cellular Ultrastructure and Virion Morphology, and Evidence*
18 *of Inducing Autophagy*. Viruses, 2019. **11**(5): p. 455.
- 19 8. Qinfen, Z., et al., *The life cycle of SARS coronavirus in Vero E6 cells*. Journal of medical
20 virology, 2004. **73**(3): p. 332-337.
- 21 9. Habibzadeh, P. and E.K. Stoneman, *The Novel Coronavirus: A Bird's Eye View*. The
22 international journal of occupational and environmental medicine, 2020. **11**(2): p. 65-71.
- 23 10. Han, W., et al., *The course of clinical diagnosis and treatment of a case infected with*
24 *coronavirus disease 2019*. Journal of medical virology, 2020: p. 10.1002/jmv.25711.
- 25 11. Special Expert Group for Control of the Epidemic of Novel Coronavirus Pneumonia of the
26 Chinese Preventive Medicine, A., *An update on the epidemiological characteristics of*
27 *novel coronavirus pneumonia (COVID-19)*. Zhonghua liu xing bing xue za zhi =
28 Zhonghua liuxingbingxue zazhi, 2020. **41**(2): p. 139-144.
- 29 12. Lipsitch, M., D.L. Swerdlow, and L. Finelli, *Defining the Epidemiology of Covid-19 -*
30 *Studies Needed*. The New England journal of medicine, 2020: p. 10.1056/NEJMp2002125.
- 31 13. Zhang, L. and Y. Liu, *Potential Interventions for Novel Coronavirus in China: A Systematic*
32 *Review*. Journal of medical virology, 2020: p. 10.1002/jmv.25707.
- 33 14. Gallagher, T.M. and M.J. Buchmeier, *Coronavirus spike proteins in viral entry and*
34 *pathogenesis*. Virology, 2001. **279**(2): p. 371-374.
- 35 15. Belouzard, S., et al., *Mechanisms of coronavirus cell entry mediated by the viral spike*
36 *protein*. Viruses, 2012. **4**(6): p. 1011-1033.
- 37 16. Li, F., *Structure, Function, and Evolution of Coronavirus Spike Proteins*. Annual review of
38 virology, 2016. **3**(1): p. 237-261.
- 39 17. Li, F., et al., *Structure of SARS coronavirus spike receptor-binding domain complexed with*
40 *receptor*. Science (New York, N.Y.), 2005. **309**(5742): p. 1864-1868.
- 41 18. Du, L., et al., *The spike protein of SARS-CoV--a target for vaccine and therapeutic*
42 *development*. Nature reviews. Microbiology, 2009. **7**(3): p. 226-236.
- 43 19. Zhou, P., et al., *A pneumonia outbreak associated with a new coronavirus of probable*
44 *bat origin*. Nature, 2020: p. 10.1038/s41586-020-2012-7.
- 45 20. Hattne, J., D. Fange, and J. Elf, *Stochastic reaction-diffusion simulation with MesoRD*.
46 Bioinformatics, 2005. **21**(12): p. 2923-4.

- 1 21. Ander, M., et al., *SmartCell, a framework to simulate cellular processes that combines*
2 *stochastic approximation with diffusion and localisation: analysis of simple networks.*
3 *Syst Biol* (Stevenage), 2004. **1**(1): p. 129-38.
- 4 22. Rodriguez, J.V., et al., *Spatial stochastic modelling of the phosphoenolpyruvate-*
5 *dependent phosphotransferase (PTS) pathway in Escherichia coli.* *Bioinformatics*, 2006.
6 **22**(15): p. 1895-901.
- 7 23. Ando, T. and J. Skolnick, *Crowding and hydrodynamic interactions likely dominate in vivo*
8 *macromolecular motion.* *Proceedings of the National Academy of Sciences of the United*
9 *States of America*, 2010. **107**(43): p. 18457-18462.
- 10 24. McGuffee, S.R. and A.H. Elcock, *Diffusion, Crowding & Protein Stability in a Dynamic*
11 *Molecular Model of the Bacterial Cytoplasm.* *Plos Computational Biology*, 2010. **6**(3).
- 12 25. Chakraborty, A.K. and A. Kosmrlj, *Statistical mechanical concepts in immunology.* *Annual*
13 *review of physical chemistry*, 2010. **61**: p. 283-303.
- 14 26. Wang, S., et al., *Manipulating the selection forces during affinity maturation to generate*
15 *cross-reactive HIV antibodies.* *Cell*, 2015. **160**(4): p. 785-797.
- 16 27. Wrapp, D., et al., *Cryo-EM structure of the 2019-nCoV spike in the prefusion*
17 *conformation.* *Science (New York, N.Y.)*, 2020: p. eabb2507.
- 18 28. Gabdoulline, R.R. and R.C. Wade, *Biomolecular diffusional association.* *Curr Opin Struct*
19 *Biol*, 2002. **12**(2): p. 204-13.
- 20 29. Zhou, H.X., *Rate theories for biologists.* *Q Rev Biophys*, 2010. **43**(2): p. 219-93.
- 21 30. Everett, H. and G. McFadden, *Apoptosis: an innate immune response to virus infection.*
22 *Trends Microbiol*, 1999. **7**(4): p. 160-5.
- 23 31. Loo, Y.M. and M. Gale, Jr., *Immune signaling by RIG-I-like receptors.* *Immunity*, 2011.
24 **34**(5): p. 680-92.
- 25 32. Subramanian, N., et al., *The adaptor MAVS promotes NLRP3 mitochondrial localization*
26 *and inflammasome activation.* *Cell*, 2013. **153**(2): p. 348-61.
- 27 33. Koshiba, T., *Mitochondrial-mediated antiviral immunity.* *Biochim Biophys Acta*, 2013.
28 **1833**(1): p. 225-32.
- 29 34. Sasaki, O., et al., *A structural perspective of the MAVS-regulatory mechanism on the*
30 *mitochondrial outer membrane using bioluminescence resonance energy transfer.*
31 *Biochim Biophys Acta*, 2013. **1833**(5): p. 1017-27.
- 32 35. Heymann, D.L., et al., *COVID-19: what is next for public health?* *Lancet* (London,
33 *England*), 2020: p. S0140-6736(20)30374-3.
- 34 36. Chen, N., et al., *Epidemiological and clinical characteristics of 99 cases of 2019 novel*
35 *coronavirus pneumonia in Wuhan, China: a descriptive study.* *Lancet* (London, England),
36 2020. **395**(10223): p. 507-513.
- 37 37. Li, Q., et al., *Early Transmission Dynamics in Wuhan, China, of Novel Coronavirus-*
38 *Infected Pneumonia.* *The New England journal of medicine*, 2020: p.
39 10.1056/NEJMoa2001316.
- 40 38. Roy, A., A. Kucukural, and Y. Zhang, *I-TASSER: a unified platform for automated protein*
41 *structure and function prediction.* *Nat Protoc*, 2010. **5**(4): p. 725-38.
- 42 39. Wan, Y., et al., *Receptor recognition by novel coronavirus from Wuhan: An analysis*
43 *based on decade-long structural studies of SARS.* *Journal of virology*, 2020: p. JVI.00127-
44 20.
- 45 40. Guerler, A., B. Govindarajoo, and Y. Zhang, *Mapping monomeric threading to protein-*
46 *protein structure prediction.* *J Chem Inf Model*, 2013. **53**(3): p. 717-25.
- 47 41. Mukherjee, S. and Y. Zhang, *Protein-protein complex structure predictions by multimeric*
48 *threading and template recombination.* *Structure*, 2011. **19**(7): p. 955-66.

2020-02-17

Multiscale Simulations of New Coronavirus

- 1 42. Xie, Z.R., J. Chen, and Y. Wu, *Predicting Protein-protein Association Rates using Coarse-*
2 *grained Simulation and Machine Learning*. *Sci Rep*, 2017. **7**: p. 46622.
- 3 43. Chen, J., S.C. Almo, and Y. Wu, *General principles of binding between cell surface*
4 *receptors and multi-specific ligands: A computational study*. *PLoS Comput Biol*, 2017.
5 **13**(10): p. e1005805.
- 6 44. Chen, J., Z.R. Xie, and Y. Wu, *Elucidating the general principles of cell adhesion with a*
7 *coarse-grained simulation model*. *Mol Biosyst*, 2016. **12**(1): p. 205-18.
- 8 45. Xie, Z.-R., J. Chen, and Y. Wu, *A coarse-grained model for the simulations of biomolecular*
9 *interactions in cellular environments*. *Journal of Chemical Physics*, 2014. **140**: p. 054112.
- 10 46. Gillespie, D.T., *Stochastic simulation of chemical kinetics*, in *Annual Review of Physical*
11 *Chemistry*. 2007, Annual Reviews: Palo Alto. p. 35-55.

12

13

14

15

16

17

18

19

20

21

22

23

24

25

26

27

28

29

30

2020-02-17

Multiscale Simulations of New Coronavirus

1 **Figure Legends**

2 **Figure 1:** A mesoscopic model is constructed to simulate the kinetic process about how
3 viruses are captured by the cell surface receptors on plasma membrane **(a)**. The plasma
4 membrane is represented by a flat surface below the extracellular region, which contains
5 a number of ACE2 receptors (pink). The space above the plasma membrane represents
6 the extracellular region which contains a number of coronaviruses (golden). Each virus is
7 simplified as a spherical rigid body with trimeric S-proteins uniformly distributed on its
8 surface (green dots). Each S-protein monomer can interact with an ACE2 receptor on the
9 plasma membrane. The rate of their association was estimated by Monte-Carlo
10 simulations based on the structure models of complexes between ACE2 and RBD
11 domains from S-proteins of different coronavirus **(b)**. The proteins in the figure are coded
12 by different color index.

13 **Figure 2:** We used structure-based kinetic Monte-Carlo simulations to estimate the
14 association between ACE2 and S-proteins from SARS-CoV and 2019-nCoV. For each
15 system, 200 simulation trajectories were generated. Based on these trajectories, the
16 calculated probabilities of association are plotted in **(a)**. We found that the association
17 between ACE2 and SARS-CoV S-proteins (right column) is faster than the association
18 between ACE2 and 2019-nCoV S-protein (left column). We then fed the information into
19 the rigid-body-based simulations. The simulations show the total numbers of viruses that
20 were captured by host cells increased as a function of simulation time **(b)**. Moreover, we
21 found that during the early stage of simulations, more SARS-CoV (black curve) attach to
22 host cells than 2019-nCoV (red curve).

23 **Figure 3:** A mathematical model was proposed to delineate the simplified process of
24 viral life cycle, including its replication and packaging in host cells, the inflammatory
25 signaling pathways due to the detection of foreign pathogens, and the follow-up
26 inflammatory responses which lead to the apoptosis of infected cells and the removal of
27 viruses by the recruitment of immune cells. The meaning of each variable in the diagram
28 is specified on the right. The system can further be described by a set of ordinary
29 differential equations, as written from Equation (1) to Equation (7) in the main text.

2020-02-17

Multiscale Simulations of New Coronavirus

1 **Figure 4:** Given predefined weights for all the rate parameters and the initial values for
2 each variable in the model, the dynamics of the system is evolved as a function of time by
3 solving the mathematical model numerically with a stochastic simulation algorithm. The
4 figure suggests that the dynamics of the system can be divided into three stages **(a)**. We
5 further applied the model to two comparative systems. A relatively fast viral binding rate
6 k_b was adopted in the first system to represent the binding process of SARS, while a
7 relatively slow rate was adopted in the second to represent the binding process of 2019-
8 nCoV. As shown in **(b)**, we found that the first stage in the simulation of 2019-nCoV (red
9 curve) is longer than the simulation of SARS (black curve), while the level of free virus
10 at the end of the first period in 2019-nCoV is relatively higher than the corresponding
11 level of free virus in SARS.

12

13

14

15

16

17

18

19

20

21

22

23

24

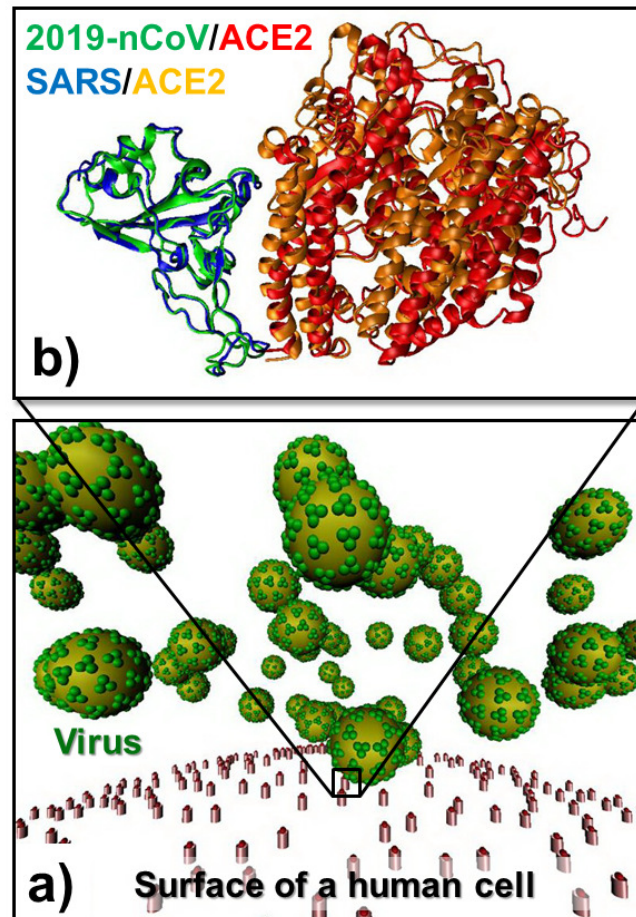
2020-02-17

Multiscale Simulations of New Coronavirus

1

2

3



4

5

6

7

8

9

10

Figure 1

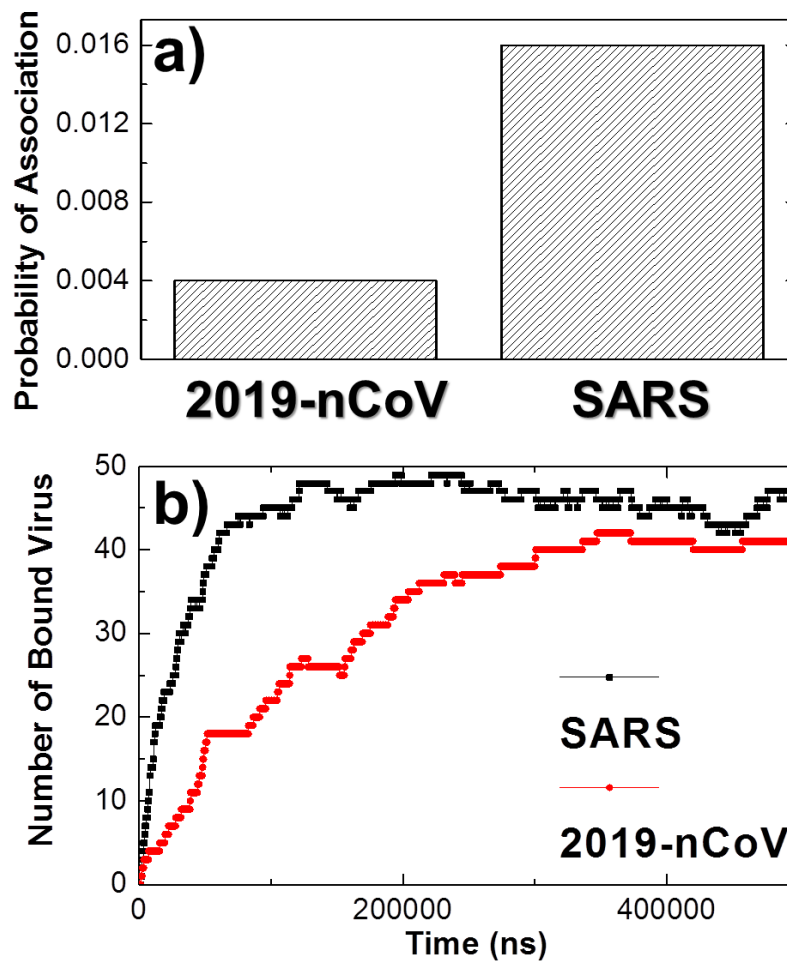
2020-02-17

Multiscale Simulations of New Coronavirus

1

2

3



4

5

6

7

8

9

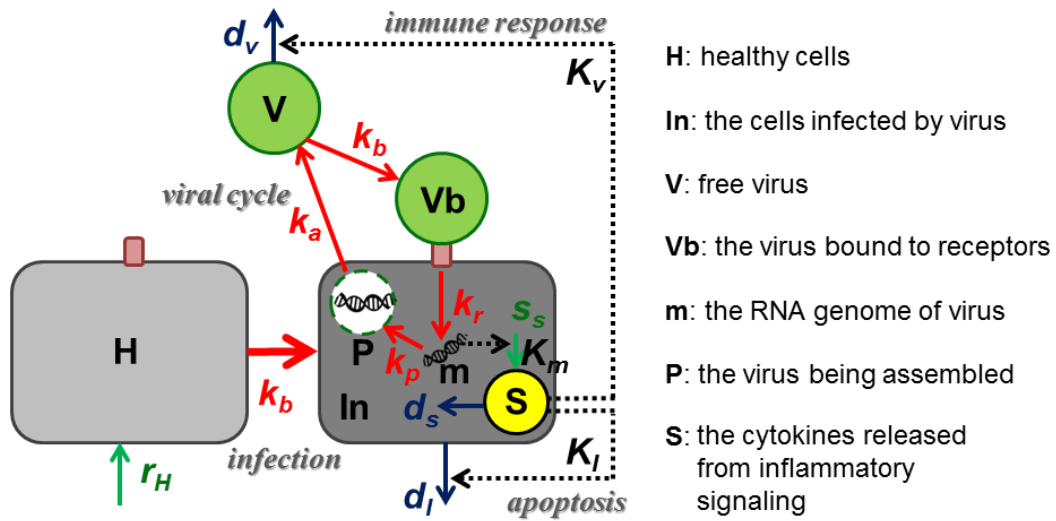
10

Figure 2

2020-02-17

Multiscale Simulations of New Coronavirus

1
2
3
4
5



6
7
8
9
10
11
12
13
14
15

Figure 3

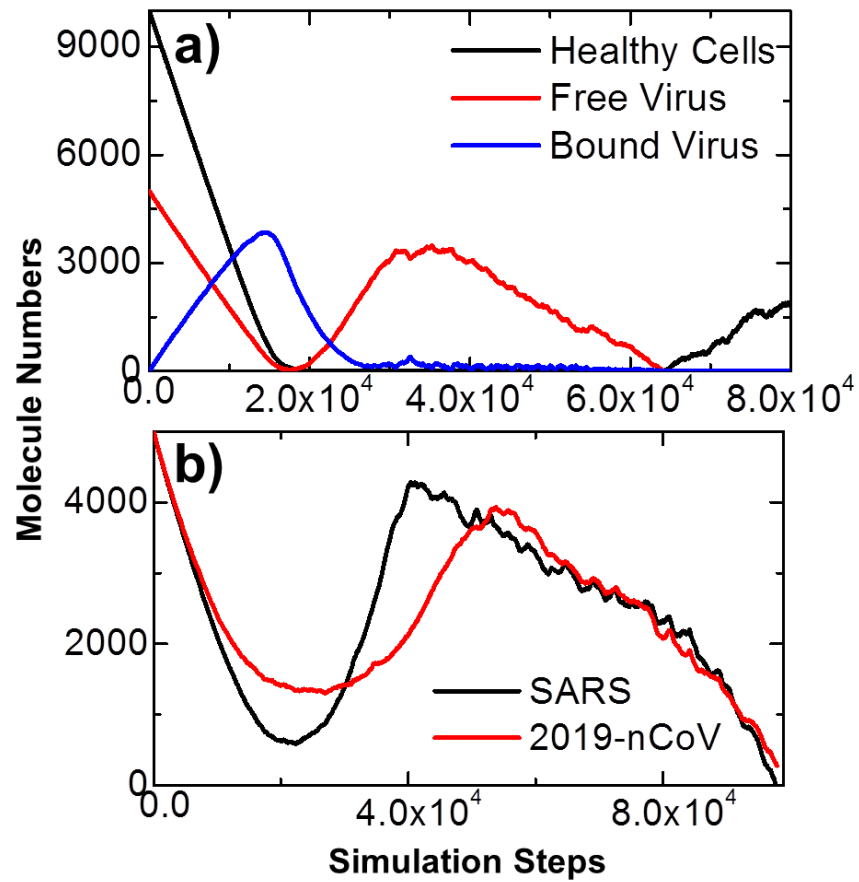
2020-02-17

Multiscale Simulations of New Coronavirus

1

2

3



4

5

Figure 4